Vibrational spectrum of reidite $ZrSiO_4$ from first principles

Mikhail B. Smirnov,[1] Sergey V. Sukhomlinov,[2] and Konstantin S. Smirnov[2]
[1]*Fock Institute of Physics, Saint-Petersburg State University, Petrodvoretz, 194508 St.-Petersburg, Russia*
[2]*Laboratoire de Spectrochimie Infrarouge et Raman, CNRS–Université Lille 1–Sciences et Technologie, 59655 Villeneuve d'Ascq, France*
(Received 17 May 2010; published 16 September 2010)

Structure, energetic characteristics, and the vibrational spectrum of reidite ($ZrSiO_4$ polymorph isostructural with sheelite) were studied by periodic density-functional calculations and compared with those of zircon. The computed structural parameters are in a good agreement with known data. The calculations provide a nonempirical estimation of the elastic constants of this material. Making use of the results of the computations a complete assignment of the phonons at the Γ point is proposed that accounts for features observed in the infrared and Raman spectra of reidite. The comparison of atomic displacements in the vibrational modes of the reidite and zircon structures permits to explain differences in their vibrational spectra in terms of structural peculiarities of the two lattices. Analysis of calculated effective charge tensors points to the validity of the two-body charge redistribution model and gives an estimation for the values of the corresponding charge transfer parameters.

DOI: 10.1103/PhysRevB.82.094307 PACS number(s): 63.20.dk, 61.50.Ah, 78.30.Hv

I. INTRODUCTION

Reidite, a metastable Scheelite-type polymorph of $ZrSiO_4$, was first discovered in the high-pressure and high-temperature experiments,[1] where the zircon (ground-state polymorph) was found to be completely converted into Scheelite-type crystal structure at $T=1200$ K and $P=12$ GPa. Later on, this structural transformation was observed in the shock wave[2,3] and in the static compression experiments at room temperature.[4,5] In the latter studies the transformation was found to begin at pressure above 20 GPa. The zircon to reidite transformation is not reversible and the reidite structure persists upon the pressure release. Nevertheless, reidite returns to the zircon structure when it is heated to 1500 K.[2]

The interest to the zirconium silicate and to the structural transformations of its polymorphs is manyfold. In the Earth's crust zirconium silicate is a host for uranium and thorium (the natural source of radiogenic heat) and the material is therefore considered as a natural storage for radioactive wastes. The measurements of the concentration of the Th and U atoms isomorphically substituting zirconium in the $ZrSiO_4$ structure is an important means of geological dating. Owing its large refractive index, zircon (like zirconia) is widely used as gemstones. Another reason of interest to this material is due to its extraordinary physical properties. High permittivity of $ZrSiO_4$ makes it a promising alternative to the conventional silicon oxide as the gate dielectric material in metal-oxide-semiconductor devices. The compressibility and thermal expansion of zircon are the lowest among the oxygen-based compounds; reidite was found to be one of the most incompressible silicate crystal.[6]

Vibrational spectroscopy is a very efficient technique for studying interatomic interactions and atomic rearrangements accompanying structural phase transformation. The vibrational states of zircon were thoroughly studied both experimentally[6–9] and theoretically[10] while significantly less attention was paid to reidite. Despite notable differences in the IR (Ref. 3) and Raman[3–5] spectra of reidite samples obtained in different experiments, no quantitative analysis of the zone-center normal vibrations of the structure and their relation to the experimental Raman and IR spectra was given. The only attempt to perform such an analysis was done using empirical potentials and the study was restricted to the analysis of total density of vibrational states.[11] No first-principles computational results were reported up to now. This paper aims to fill this gap by reporting results of *ab initio* study of the reidite vibrational spectrum. Given the chemical and structural similarity of reidite and zircon, the latter structure was also investigated using the same approach; the outcome of this investigation serves as a basis for the discussion of the results on reidite.

II. COMPUTATIONAL PROCEDURE

The first-principle periodic calculations of the reidite and zircon structures were performed in the framework of density-functional theory (DFT) as implemented in the CRYSTAL06 code.[12] We used Becke's three-parameter hybrid nonlocal exchange functional combined with Lee-Yang-Parr gradient-corrected correlation functional (B3LYP). The use of this functional in periodic quantum-chemical calculations was found to result in an accurate description of the structural data,[13] electronic structure,[14] and dielectric properties of different materials.[15] The application of B3LYP for studying the vibrational dynamics of simple[16,17] and complex oxides[18] has shown that the phonon frequencies can be reproduced with a precision better than 10 cm^{-1}. In the present study the atoms were described with all-electron basis sets. The basis sets reported in Refs. 19 and 20 were used for the Si and O atoms, respectively. The basis set for the Zr atom was taken from Ref. 21 and optimized to minimize the energy of zircon structure with the lattice parameters and atomic positions fixed at the experimental values.

The Brillouin zone integration was done over a Monkhorst-Pack grid of $6\times6\times6$ k points, the energy convergence criterium in the self-consistent-field procedure was set to 10^{-10} Ha. Zero-pressure and zero-temperature struc-

TABLE I. Structural parameters (in Å) of reidite and zircon crystalline lattices and fractional coordinates of oxygen atoms in the primitive cells.

	Reidite					Zircon				
Method, Ref.	a	c	x/a	y/a	z/c	a	c	x/a	y/a	z/c
Expt.[a]	4.734	10.510	0.28	0.14	0.07	6.61	6.00	0.0	0.1854	0.1783
LDA[b]	4.723	10.411	0.2585	0.1573	0.0788	6.599	5.959	0.0	0.1839	0.1806
LDA[c]						6.54	5.92	0.0	0.1855	0.1805
GGA[b]	4.788	10.640	0.2584	0.1571	0.0774	6.704	6.040	0.0	0.1833	0.1797
GGA[d]	4.722	10.629	0.2572	0.1550	0.0757	6.632	5.987	0.0	0.1828	0.1763
B3LYP, this work	4.776	10.620	0.2583	0.1561	0.0772	6.679	6.044	0.0	0.1824	0.1799

[a]Experimental data for reidite and zircon from Refs. 23 and 24, respectively.
[b]Reference 25.
[c]Reference 10.
[d]Reference 26.

tures of the two crystalline $ZrSiO_4$ polymorphs were obtained in a complete geometry optimization. The residual atomic forces in the final structures were less than 7×10^{-7} and 4×10^{-6} Ha Bohr^{-1} for the zircon and reidite lattices, respectively, and the frequencies of three low-energy acoustic modes (≤ 2 cm^{-1}) indicated that the energy minimum was indeed achieved.

The infrared spectrum of reidite was computed taking the transversal-longitudinal (TO-LO) splitting for the polar vibrational modes into account. The dielectric tensor components for the reidite structure $\epsilon_\infty^\perp=3.883$ and $\epsilon_\infty^\parallel=3.807$ were obtained in the CRYSTAL06 calculations (the signs $\perp$ and $\parallel$ denote the dielectric tensor components in the directions perpendicular and parallel to the c axis, respectively).[22]

III. RESULTS AND DISCUSSION

A. Structure

The optimized structural parameters of reidite and zircon lattices are compared in Table I with the available experimental data and with the results of other computational studies performed within the DFT with the plane-waves-basis set. It is seen that the calculations reported in this paper well reproduce the geometry of both structures; a slight overestimation of the unit-cell linear dimensions (approximately 1%) occurs for both the reidite and zircon lattices. The table shows that the calculations based on local density approximation (LDA) systematically underestimate the unit cell dimensions, whereas results obtained in the calculations using generalized gradient approximation (GGA) do not reveal such a regular behavior. Nevertheless, all the DFT calculations predict the reidite/zircon volume ratio equal to 0.9 that is in a good agreement with the experimental data.[4,5,27]

B. Energy characteristics

As previous computational studies[26,28,29] the present calculations give the zircon structure as the lowest energy polymorph of $ZrSiO_4$. However, the energy difference $\Delta E = E(\text{reidite}) - E(\text{zircon})$ obtained in these calculations are markedly different, as illustrated in Table II. It is remarkable that the ΔE values predicted by the GGA calculations are twice as large as those obtained in the LDA calculations. The present B3LYP study gives the energy difference value which is between the GGA and LDA results. The same tendency is seen for the critical pressure P_C, whose values derived from the enthalpy equalization condition are listed in the last column of Table II. Unfortunately, both the ΔE and P_C quantities cannot be obtained from the available experimental data because of a highly pronounced first-order character of the zircon-to-reidite transformation.

C. Elastic constants and bulk moduli

Table III reports calculated values of the elastic constants and bulk moduli for reidite and zircon, and compares them with the experimental data and results of previous calculations. The comparison with the experimental data for zircon shows an overall good agreement, especially for the constants C_{11}, C_{44}, and C_{12}. Measured values of the bulk modulus for zircon differ from each other by approximately 10%. The bulk modulus obtained in our calculations is close to the upper limit of these values and agrees well with the experi-

TABLE II. Equilibrium volume V (in Å^3/molecule), reidite-zircon energy difference ΔE (in eV/molecule), and critical pressure P_C (in GPa).

Method, Ref.	V(reidite)	V(zircon)	ΔE	P_C
Expt.[a]	58.884	65.538		
LDA[b]	58.059	64.874	0.217	5.3
LDA[c]	58.0	64.5	0.205	5
GGA[b]	60.980	67.865	0.482	11.2
GGA[d]	59.249	65.832	0.598	15
B3LYP, this work	60.571	67.405	0.345	8.7

[a]Experimental data for reidite and zircon from Refs. 23 and 24, respectively.
[b]Reference 25.
[c]Reference 28.
[d]Reference 26.

TABLE III. Elastic constants C_{ij} and bulk modulus B_0 (in GPa) of reidite and zircon structures.

	C_{11}	C_{33}	C_{44}	C_{66}	C_{12}	C_{13}	C_{16}	B_0
				Reidite				
B3LYP, this work	467.0	364.6	109.2	157.2	202.7	168.5	97.0	258.5
Expt.[a]								301.4 ± 12.5
Expt.[b]								392 ± 9
LDA[c]								258
GGA[c]								221
Eff. potentials[d]	470	288	74	133	241	255		303
				Zircon				
B3LYP, this work	427.5	509.8	110.1	41.2	69.9	169.0	0	233.6
Expt.[e]	424.4	489.6	113.3	48.2	69.2	150.2		227.6
Expt.[f]								199 ± 1
Expt.[b]								205 ± 8
Expt.[c]								225 ± 8
Expt.[g]								227 ± 2
LDA[c]								231
GGA[c]								201

[a]Reference 6.
[b]Reference 30.
[c]Reference 25.
[d]Reference 11.
[e]Reference 31.
[f]Reference 5.
[g]Reference 32.

mental and theoretical results by Marqués *et al.*[25]

The available experimental B_0 values for reidite have even larger scatter, up to 27%. Results of the present calculations are closer to the value 301.4 ± 12.5 GPa obtained by Scott *et al.*[6] and, as the other nonempirical calculations do,[25] underestimate the measured bulk modulus of this material. There are no experimental data on the elastic constants of reidite; to the best of our knowledge the data presented in Table III provide the theoretical prediction based on nonempirical calculations. Elastic constants for reidite were calculated by Chaplot *et al.*[11] using empiric model potentials. Comparison of their results with our data (Table III) shows the same trend for values of the diagonal constants while absolute values differ significantly.

D. Phonons

1. Phonons: General considerations

Space symmetry group of reidite is $I4_1/a$ (C_{4h}^6). There are 12 atoms (two formula units) in the primitive cell and the zone-center normal modes are distributed over irreducible symmetry representations as follows:

$$\Gamma = 3A_g + 5B_g + 5E_g + 5A_u + 3B_u + 5E_u.$$

The $ZrSiO_4$ compound can roughly be considered as an orthosilicate of zirconium. From this view point, its crystal structure consists of Zr^{4+} cations and silicate anions $[SiO_4]^{4-}$. Correspondingly, the normal modes of such a structure in the center of Brillouin zone can be classified in terms of relative translations of cations and anions, rotations, and internal vibrations of the complex anions. The internal vibrations of an isolated regular SiO_4 tetrahedron are characterized by four modes of different symmetry, which are depicted in Fig. 1. These are totally symmetric bond-stretching mode (ν_1), triply degenerated antisymmetric bond-stretching mode (ν_3), triply degenerated umbrellalike angle-bending mode (ν_4), and doubly degenerated angle-bending scissoring mode (ν_2). For both the zircon and reidite crystal lattices the presence of the inversion symmetry operation, which transforms the two translationally nonequivalent structural units one to other, further facilitates the analysis of normal modes. Thus, any mode of even parity (*gerade*) includes in-phase deformations or antiparallel displacements of SiO_4 tetrahedra while any mode of uneven parity (*ungerade*) involves antiphase deformations or parallel displacements of the tetrahedra. All vibrational modes can then be sorted into twin pairs consisting of the corresponding tetrahedra motions. Furthermore, assuming relatively weak intertetrahedra interactions, one can

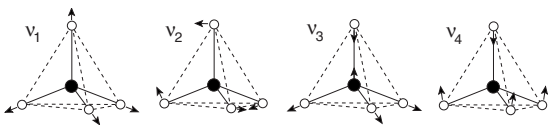

FIG. 1. Schematic presentation of internal vibrations of isolated tetrahedron.

TABLE IV. Frequencies and assignment of zone-center phonons of reidite according to DFT calculations. The corresponding data for zircon structure are given for comparison.

Reidite		Zircon			
A_g	B_u	A_g	B_u	Assignment	Raman peak[a]
875	*848*[b]	981 (1)[c]	*960* (2)	ν_1	1
420	*656*	464 (1)	*606* (2)	ν_2^z	6
334	*404*	*251* (2)	*141* (1)	R_z	8
B_g	A_u	B_g	A_u		
852	791	1017 (1)	983 (2)	ν_3^z	2
635	625	666 (1)	617 (2)	ν_4^z	3
483	376	262 (2)	*449* (1)	ν_2^{xy}	5
362	0	230 (1)	0 (2)	T_z^+	10
247	290	407 (1)	363 (2)	T_z^-	7
E_g	E_u	E_g	E_u		
893	848	921	865	ν_3^x, ν_3^y	1
570	513	574	439	ν_4^x, ν_4^y	4
469	381	366	404	R_x, R_y	5
301	250	239	286	T_x^-, T_y^-	9
214	0	204	0	T_x^+, T_y^+	11

[a]Figure 5.
[b]Frequencies of silent modes are given in italic.
[c]Numbers in parentheses show different symmetry species A_{1g}, A_{2g}, etc.

suppose that the frequencies of such twin modes do not significantly differ from each other. These two issues will further be used while analyzing the vibrational dynamics of the lattices.

One of reasons of splitting of the internal vibrations of tetrahedral units in crystals is their distortion lifting the degeneracy. In the reidite structure the SiO_4 tetrahedra are flattened in z direction and the mode splitting predicted from the geometric consideration is as follows. The tetrahedron vibrations polarized in x an y directions (E modes of crystal originating from ν_3^x and ν_3^y tetrahedron vibrations) must have higher frequencies than the same vibrations polarized in z direction (A and B modes coming from ν_3^z vibration). In contrast, the E modes coming from the ν_4 vibration must have lower frequencies than the analogous A and B modes. The structural distortion of the tetrahedra also affects the two ν_2 vibrations: that involving elongation of tetrahedron in z direction (ν_2^z) must have lower frequency than another one producing tetrahedron deformation in the xy plane (ν_2^{xy}). Note that in zircon structure, the tetrahedra are elongated in the z direction and consequently, one can expect an opposite character of the distortion-induced splitting.

The calculated modes of the reidite and zircon structures classified according to the twin scheme by the analysis of the calculated eigenvectors at the Γ point are listed in Table IV; the corresponding motions of the SiO_4 tetrahedra are reported in the next to the last column of the table with the polarization of the modes of SiO_4 tetrahedra shown by the upper index. For the rotational (R) and translational (T) modes the Cartesian subindex denotes orientation of the rotational axes or direction of the translation. Signs plus and minus in notations of translations serve to discriminate between in-phase and antiphase translations of cations and anions located in the same ab plane. The results of present calculations on zircon are in a good agreement with those of Ref. 10.

2. Phonons: Discussion

The results given in Table IV show that the calculated frequencies of the ν_2, ν_3, and ν_4 modes of reidite follow the splitting rules predicted above by considering the distortion of the SiO_4 tetrahedra in the structure. It can also be seen that the assumption of weakly interacting tetrahedra seems to be reasonable for the high-frequency modes coming from ν_1 and ν_3 tetrahedron vibrations. For these modes, the g-u frequency splitting does not exceed 60 cm^{-1} (i.e., less than 8% of the frequency value). Moreover, a decrease in frequencies of polar A_u and E_u modes with respect to the corresponding B_g and E_g twins can be partly explained by Lorentz field effect.

At the same time, Table IV shows that the g-u splitting is significant for some modes coming from ν_2 and ν_4 tetrahedron vibrations. In zircon, the maximum frequency difference is observed for the B_{2u} (ν_2^z) and A_{1g} (ν_2^z) modes and it amounts to 142 cm^{-1}. In reidite, the frequency differences between B_u (ν_2^z) and A_g (ν_2^z) modes is larger and achieves 236 cm^{-1}. Such a large difference suggests that these modes

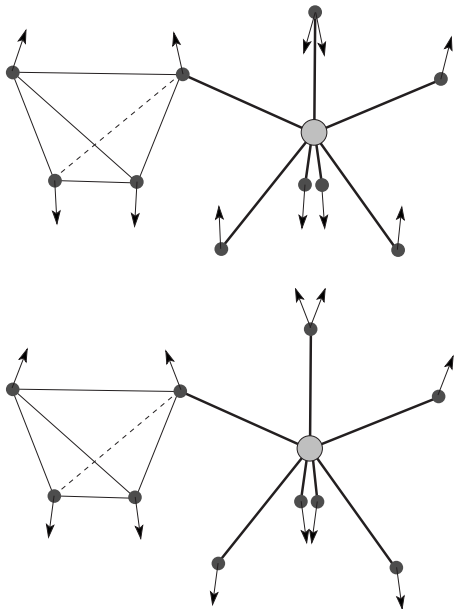

FIG. 2. Displacements of atoms in A_g mode at 420 cm^{-1} (top) and in B_u mode at 656 cm^{-1} (bottom) of reidite structure. Small gray circles and large gray circle denote oxygen and zirconium atoms, respectively.

cannot be considered as local vibrations of isolated tetrahedra. Previous *ab initio* calculations of ZrO_2 polymorphs[33] indicated that modes involving stretching vibrations of Zr-O bonds lie in the frequency interval from 500 to 600 cm^{-1}. Hence, the modes in the region 450–650 cm^{-1} usually classified as either the ν_2 or ν_4 tetrahedron vibrations[3,4,34] can have an important contribution of Zr-O bond stretching coordinates.

Let us consider in more details the *g*-*u* twins related to ν_2^z vibrations in reidite: the A_g mode at 420 cm^{-1} and the B_u mode at 656 cm^{-1}. The calculated atomic displacements of these modes are shown in Fig. 2. It is clearly seen that both the modes involve similar deformations of the SiO_4 tetrahedra. The phase difference in these modes, however, produces markedly different distortions of the ZrO_8 polyhedra. The polyhedra accomplish quasi-isotropic pulsations in the B_u mode whereas in the A_g mode the distortion of the ZrO_8 polyhedrons is more complicated: a half of Zr-O bonds shorten while the other half of the bonds stretch. Furthermore, as Fig. 2 illustrates, the B_u mode involves an important variation of the lengths of the O-O edges in the ZrO_8 polyhedra whereas the A_g mode does not. Hence, the different behavior of the Zr-O and of O-O distances in these modes permits to explain such a large *g*-*u* frequency splitting.

The zirconium-oxygen interactions also result in relatively high frequencies of modes, which are nominally attributed to tetrahedron rotations (R) and translations (T). Thus, the frequency 404 cm^{-1} of the lowest B_u mode in reidite, which can be described as R_z mode, is comparable with frequencies of intratetrahedron modes. Computed eigenvector of the R_z mode is shown in Fig. 3 (top panel). It is clearly seen that this mode indeed produces rotation of SiO_4 tetrahedra. At the same time, this motion leads to the shortening of a half of the Zr-O bonds. These are just these deformations that account for such a relatively high frequency of the mode classified as the tetrahedron rotation. It is worthy of note that in zircon the same mode (B_{1u}) has much lower frequency 141 cm^{-1}. This result can be explained by structural difference between the two lattices. The computed eigenvector of the B_{1u} mode in zircon is displayed in Fig. 3 (bottom panel). One sees that this mode involving pure rotations of SiO_4 tetrahedrons also produces quasirotations of the ZrO_8 polyhedrons without changing the Zr-O bond lengths.

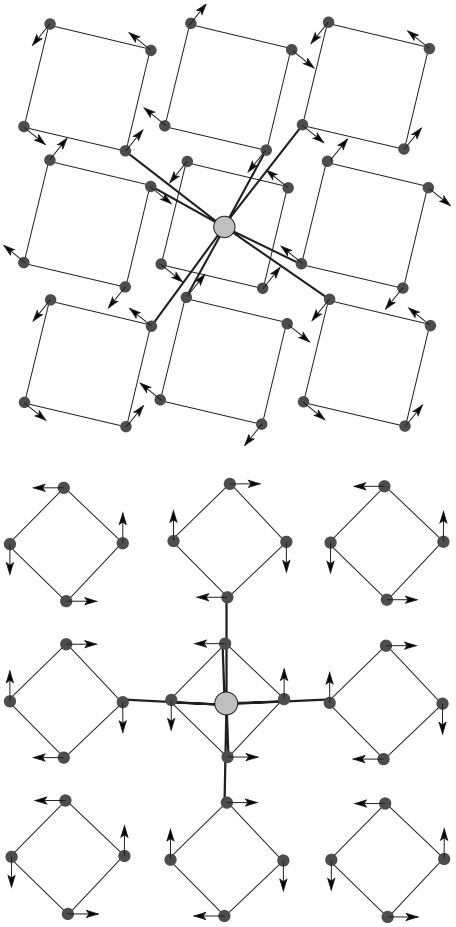

FIG. 3. Displacements of atoms in B_u mode at 404 cm^{-1} of reidite (top) and in B_{1u} mode at 141 cm^{-1} of zircon (bottom). Tetrahedra SiO_4 are shown as squares with oxygen atoms in corners; large gray circle in the center of figures denote zirconium atom.

Analysis of Table IV shows that the A and B modes (ν_1 and ν_3^z) of reidite structure have notably lower frequencies than those of zircon one (downward shift amounts to 192 cm^{-1}) while frequencies of the E modes do not differ significantly from each other. This feature results from a common action of two factors. The first one is a decrease in Si-O force constant due to an increase in the Si-O bond length in reidite as compared to that in zircon. Our calculations predict the Si-O bond lengthening from 1.633 to 1.658 Å, in a good agreement with the change from 1.623 to 1.655 Å found experimentally.[23] An estimation based on the Badger rule[35] shows that the increase of the bond length can account for a downward shift of ~60 cm^{-1} for the modes of the reidite structure. The second factor is the distortion of the SiO_4 tetrahedra in reidite and zircon. As it was discussed

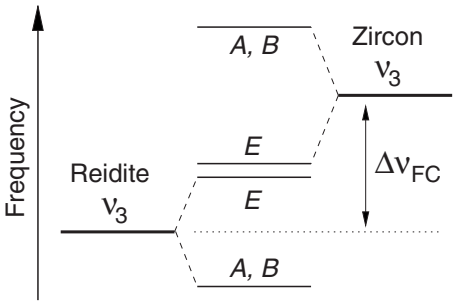

FIG. 4. Scheme illustrating splitting of the ν_3 mode of SiO_4 tetrahedra in the reidite and zircon structures. $\Delta\nu_{FC}$ stands for the frequency decrease due to the lengthening of the Si-O bonds in reidite (see text for discussion).

above (Sec. III D 1), the flattening of the tetrahedra in the z direction in reidite leads to the splitting of the triply degenerated ν_3 mode in such a way that the modes of E symmetry have higher frequencies than the modes of the A and B symmetries whereas the splitting has the opposite character in the zircon structure. As a result, while comparing two structures, the energies of E modes approach each other, while those of A and B modes are moving further apart. This issue is schematically illustrated in Fig. 4.

3. Raman and infrared spectra

Nonpolarized Raman spectra of reidite samples obtained in the high-pressure recovery experiments were reported in Refs. 3–5. Figure 5 compares an experimental Raman spectrum with frequency positions of the calculated Raman active normal modes. A proposed assignment of the observed peaks in the spectrum is presented in the last column of Table IV.

Analysis of the experimental Raman spectra of reidite reported in Refs. 4 and 5 shows that all these spectra contain peaks in the vicinity of 1000 cm^{-1}. These peaks have a notable intensity in the spectrum reported by Knittle *et al.*[4] while they are much less pronounced in the spectrum by van Westrenen *et al.*[5] and are rather weak in the spectra by Gucsik *et al.*[3] The authors of Refs. 3 and 5 suggested that these spectral features do not belong to reidite but are due the rest of zircon structure persisting in the samples because of in-

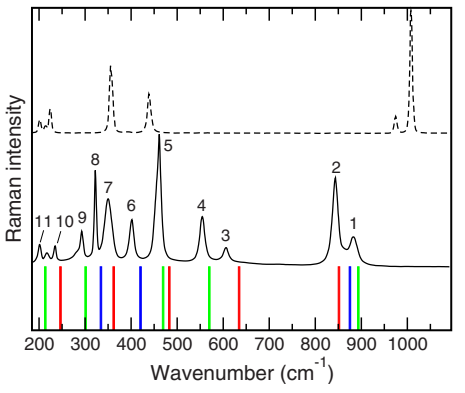

FIG. 5. (Color online) Calculated frequency positions of Raman active modes of reidite (A_g—blue, B_g—red, and E_g—green). Continuous and dashed lines show experimental spectra of reidite and zircon, respectively (adapted from Fig. 3 of Ref. 3). Digits correspond to assignment of peaks in reidite spectrum given in Table IV.

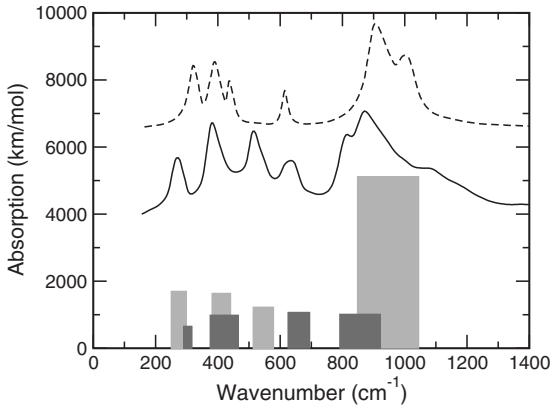

FIG. 6. Calculated IR spectrum of reidite. Gray and dark gray bars denote to E_u and A_u modes, respectively. The left side of each bar is at the position of the TO mode and the width of bar corresponds to the TO-LO splitting. The experimental powder absorption spectra of reidite (solid line) and zircon (dashed line) are shown for comparison (adapted from Fig. 1 of Ref. 3).

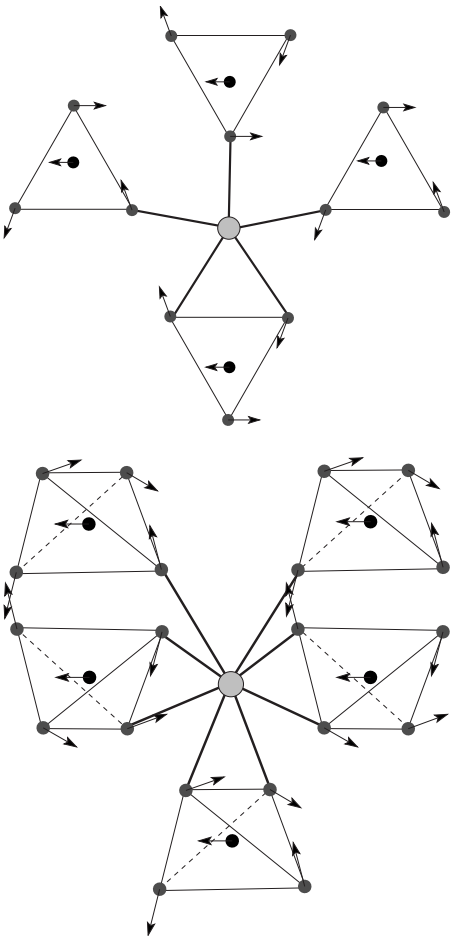

FIG. 7. Displacements of atoms in the E_u (ν_4^x) mode at 439 cm^{-1} of zircon (top) and 513 cm^{-1} of reidite (bottom). Circles in the center of the tetrahedra denote silicon atoms.

TABLE V. Calculated effective charge tensors for atoms in reidite and zircon (in e units).

Atom	Zircon[a]						Reidite		
Zr	5.527	0.000	0.000	5.41	0.00	0.00	5.095	1.349	0.000
	0.000	5.527	0.000	0.00	5.41	0.00	−1.349	5.095	0.000
	0.000	0.000	4.724	0.00	0.00	4.63	0.000	0.000	5.207
Si	3.291	0.000	0.000	3.25	0.00	0.00	4.349	−1.235	0.000
	0.000	3.291	0.000	0.00	3.25	0.00	1.235	4.349	0.000
	0.000	0.000	4.583	0.00	0.00	4.42	0.000	0.000	3.404
O	−1.254	0.000	0.000	−1.15	0.00	0.00	−2.355	−0.569	−0.400
	0.000	−3.146	0.352	0.00	−3.17	0.34	−0.569	−2.376	0.387
	0.000	0.136	−2.324	0.00	0.16	−2.25	−0.318	0.214	−2.157

[a]Tensors in parentheses are from Ref. 10.

complete phase transition. Both the studies reported a downward shift of more than 100 cm^{-1} for the high-frequency Raman peaks just after zircon-reidite phase transition. Results of our calculations permit to attribute the peaks observed around 850–900 cm^{-1} to the three high-frequency Raman modes of reidite thus confirming the assignment proposed by Westernen *et al.*[5] and by Gucsik *et al.*[3] As discussed above, the reason for the downward shift is the changes in the geometry of the SiO_4 tetrahedra upon the zircon-reidite transition that leads to the increase in the Si-O bond length. It is worth of noting that similar downward shift of the high-frequency spectral peaks in the Raman spectra was observed in studying the zircon-to-sheelite transformations of vanadates[36,37] and chromates.[38]

Figure 6 presents the spectrum of infrared active modes of reidite and compares it with the experimental absorption IR spectrum adapted from Ref. 3. Since the maxima of bands in the IR absorption spectrum lie in-between the TO-LO peaks positions, the agreement with the experimental data can be considered as very satisfactory.

Comparing the experimental IR spectra of reidite and zircon (Fig. 6) one can make some interesting observation. Indeed, the IR spectrum of reidite contains an intense band at 500 cm^{-1} that is absent in the spectrum of zircon. According to our calculations this band can be assigned to the E_u (ν_4^x) vibration and the calculated frequency of this mode is 513 cm^{-1} and 439 cm^{-1} in the reidite and zircon structures, respectively. In a line with discussion presented in Sec. III D 2, the reason for the 74 cm^{-1} frequency difference can be ascribed to the different participation of the Zr-O bonds in the vibrations.

The calculated eigenvectors of the mode in the two structures (Fig. 7) evidence that the direction of atomic displacements in the E_u (ν_4^x) mode of zircon (Fig. 7, top panel) is almost perpendicular to the Zr-O bonds and thus, the lengths of Zr-O bonds almost do not vary in the mode. On the other hand, the oxygen atom displacements in the analogous mode of reidite (Fig. 7, bottom panel) are directed along one Zr-O bond of the Zr-O-Zr bridges. Consequently, the effective force constant of this mode in reidite is enhanced because of the stretching of the Zr-O bonds.

4. Born effective charges

Table V presents the Born charge tensors $\mathbf{Z}^*$ obtained in the *ab initio* calculations for the reidite and zircon structures. Values of the effective charges evidence that the polarization in zirconium silicate polymorphs cannot be adequately described within the rigid ion approximation and that atomic displacements produce an important redistribution of electronic density, i.e., charge transfer between atoms.

Hereafter, we attempt to reveal a possible microscopic mechanism of the charge transfer. This issue was previously

TABLE VI. Effective charge tensors for atoms in the zircon and reidite structures computed with the two-body charge-transfer model.

Atom	Zircon			Reidite		
Zr	5.500	0.000	0.000	5.378	0.000	0.000
	0.000	5.500	0.000	0.000	5.378	0.000
	0.000	0.000	4.780	0.000	0.000	5.024
Si	3.253	0.000	0.000	3.999	0.000	0.000
	0.000	3.253	0.000	0.000	3.999	0.000
	0.000	0.000	4.495	0.000	0.000	3.002
O	−1.258	0.000	0.000	−2.576	−0.882	−0.635
	0.000	−3.118	0.927	−0.882	−2.113	−0.101
	0.000	0.927	−2.319	−0.635	−0.101	−2.007

TABLE VII. Parameters of two-body charge-transfer model.

Atom	Z^0 (e)	Bond[a]	C_{ij} (e)
Si	1.224	Si-O (1.633)	1.833
Zr	3.812	Zr-O (2.154)	0.789
O	−1.259	Zr-O (2.277)	0.297

[a]Bond lengths (in Å) are given in parentheses.

discussed in relation to the IR intensities of zircon in Ref. 39, where it was shown that the intensities of all IR-active modes can be satisfactorily described by assuming a two-center character of the dynamic charge transfer with the charge flow proportional to the variations in the Si-O and Zr-O bond lengths. This idea goes back to the pioneering paper by Kleinmann and Spitzer[40] and it is used here to interpret the results of the quantum-chemical calculations. The two-center charge-transfer model represents effective Born charge of atom i as

$$\mathbf{Z}_i^* = Z_i^0 \mathbf{I} + \sum_{j \in \text{bonds}} C_{ij} \mathbf{b}_{ij}, \tag{1}$$

where Z_i^0 denotes a permanent (ionic) charge of the atom, $\mathbf{I}$ is the identity tensor, C_{ij} is a charge-transfer parameter for the bond between the atoms i and j, and $\mathbf{b}_{ij}=\mathbf{e}_{ij}\otimes\mathbf{e}_{ij}$ is dyadic product of the unit vector $\mathbf{e}_{ij}$ of the bond. Obviously, the relation $C_{ij}=-C_{ji}$ should hold to maintain the electroneutrality condition. As the sign of C_{ij} parameters is ambiguous, we have chosen the positive sign for i=Zr,Si. Such a choice corresponds to the increase of cation charges upon increasing the cation-oxygen bond length and leads to the relation $\frac{1}{3}\mathrm{Tr}(\mathbf{Z}_i^*) > Z_i^0$ in agreement with the first principles results (Table V).

Considering three Z_i^0 ionic charges and three C_{ij} parameters for the Si-O and two nonequivalent Zr-O bonds, we have fitted their values in order to reproduce (in the least mean-square sense) the effective charge tensors given in Table V for atoms in the zircon polymorph. The effective charge tensors calculated with these parameters for atoms in zircon are listed in the second column of Table VI while obtained values of Z_i^0 and C_{ij} parameters are given in Table VII. It is seen that all seven diagonal $Z_{\alpha\alpha}^*$ ($\alpha=x,y,z$) values are well reproduced with five independent Z_i^0 and C_{ij} parameters. Values of the nondiagonal Z_{yz}^* element for oxygen atom are slightly overestimated. The fitted values of the Z^0 and C_{ij} parameters are realistic both from point of view of ionic charge distribution (Z_i^0 values) in the compound and from the point of view of the relative bond strengths: the C_{ij} parameters values correlate with the length and strength of the M-O bonds.

The effective charge tensors of atoms in reidite computed with the Z_i^0 and C_{ij} parameters derived on zircon are reported in the third column of Table VI. From the comparison of Tables V and VI one sees that the model well reproduces all main changes of the $\mathbf{Z}^*$ tensor elements induced by the zircon to reidite structural transformation. It can therefore be concluded that these changes are primarily due to the structural changes upon the phase transition. It is worth of noting the deviation of the symmetry of $\mathbf{Z}^*$ tensors with respect to the Cartesian indexes (Table V). This effect is more prominent for the $\mathbf{Z}^*$ tensors of atoms in the reidite structure. For the Si and Zr atoms the relation $Z_{xy}^*=-Z_{yx}^*$ is dictated by the symmetry constraint and since the two-body charge-transfer model implies the relation $Z_{xy}^*=Z_{yx}^*$, the presence of nonzero Z_{xy}^* elements points to the existence of many-body charge-transfer channels. A limitation of the two-center model also manifests itself in asymmetric values of the off-diagonal $Z_{\alpha\beta}^*$ elements for the oxygen atoms. Despite these minor discrepancies the results presented above unambiguously show that the charge transfer in the zirconium silicate polymorphs has primarily two-body character.

IV. CONCLUSIONS

The structure and phonon states at Γ point of reidite (zirconium silicate polymorph isostructural with Sheelite) were studied using periodic density-functional calculations and compared with those of zircon. Results of the calculations well agree with all structural, energetic, and dynamical properties of the zircon and reidite available in the literature. In particular, the paper reports a theoretical *ab initio* determination of the elastic constants for the reidite structure.

The results of the calculations permitted a reliable assignment of the vibrational normal modes of the reidite. The simulated vibrational spectra of both reidite and zircon polymorphs are in a good agreement with their experimental IR and Raman spectra. The results provide a definitive interpretation of the high-frequency part of the reidite vibrational spectrum and confirm the attribution of spectral features above 900 cm^{-1} in Raman spectrum to remaining untransformed domains of zircon, as it was proposed in Refs. 3 and 5. The comparison of calculated eigenvectors of the vibrational modes for the reidite and zircon structures permits to explain differences in their vibrational spectra in terms of structural peculiarities of the two lattices. Analysis of calculated effective charge tensors provides a definitive conclusion on reliability of the two-body charge redistribution model and gives estimation for corresponding charge-transfer parameters.

ACKNOWLEDGMENTS

M.B.S thanks the CNRS for support. S.V.S gratefully acknowledges support from Ministère de l'Education Nationale, de la Recherche et de la Technologie.

[1] A. F. Reid and A. E. Ringwood, Earth Planet. Sci. Lett. **6**, 205 (1969).
[2] K. Kusaba, Y. Syono, M. Kikuchi, and K. Fukuoka, Earth Planet. Sci. Lett. **72**, 433 (1985).
[3] A. Gucsik, M. Zhang, C. Koeberl, E. K. H. Salije, S. A. T. Redfern, and J. M. Pruneda, Mineral. Mag. **68**, 801 (2004).
[4] E. Knittle and Q. Williams, Am. Mineral. **78**, 245 (1993).
[5] W. van Westrenen, M. R. Frank, J. M. Hanchar, Y. Fei, R. J. Finch, and C.-S. Zha, Am. Mineral. **89**, 197 (2004).
[6] H. P. Scott, Q. Williams, and E. Knittle, Phys. Rev. Lett. **88**, 015506 (2001).
[7] P. Dawson, M. M. Hargreave, and G. R. Wilkinson, J. Phys. C **4**, 240 (1971).
[8] R. W. G. Syme, D. J. Lockwood, and H. J. Kerr, J. Phys. C **10**, 1335 (1977).
[9] B. A. Kolesov, C. A. Geiger, and T. Armbruster, Eur. J. Mineral. **13**, 939 (2001).
[10] G.-M. Rignanese, X. Gonze, and A. Pasquarello, Phys. Rev. B **63**, 104305 (2001).
[11] S. L. Chaplot, L. Pintschovius, N. Choudhury, and R. Mittal, Phys. Rev. B **73**, 094308 (2006).
[12] R. Dovesi, V. R. Saunders, C. Roetti, R. Orlando, C. M. Zicovich-Wilson, F. Pascale, B. Civalleri, K. Doll, N. M. Harrison, I. J. Bush, Ph. D'Arco, and M. Llunell, *CRYSTAL06 User's Manual* (University of Torino, Torino, 2006).
[13] A. D. Rowan, C. H. Patterson, and L. V. Gasparov, Phys. Rev. B **79**, 205103 (2009).
[14] J. Muscat, A. Wander, and N. M. Harrison, Chem. Phys. Lett. **342**, 397 (2001).
[15] M. B. Yahia, E. Orhan, A. Beltran, O. Masson, T. Merle-Méjean, A. Mirgorodski, and P. Thomas, J. Phys. Chem. B **112**, 10777 (2008).
[16] C. M. Zicovich-Wilson, F. Pascale, C. Roetti, V. R. Saunders, R. Orlando, and R. Dovesi, J. Comput. Chem. **25**, 1873 (2004).
[17] D. A. Daramola, M. Muthuvel, and G. G. Botte, J. Phys. Chem. B **114**, 9323 (2010).
[18] Y. Noel, M. Catti, Ph. D'Arco, and R. Dovesi, Phys. Chem. Miner. **33**, 383 (2006).
[19] F. Pascale, C. M. Zicovich-Wilson, R. Orlando, C. Roetti, P. Ugliengo, and R. Dovesi, J. Phys. Chem. B **109**, 6146 (2005).
[20] C. Gatti, V. R. Saunders, and C. Roetti, J. Chem. Phys. **101**, 10686 (1994).
[21] Web-site of CRYSTAL06 program, http://www.crystal.unito.it/Basis_Sets/zirconium.html
[22] CRYSTAL06 calculations for zircon have resulted in values $\epsilon_\infty^\perp = 3.394$ and $\epsilon_\infty^\parallel = 3.749$ that are in a good agreement with the available experimental data $\epsilon_\infty^\perp = 3.5$ (Ref. 41) $\epsilon_\infty^\parallel = 3.8$ (Ref. 42).
[23] K. Kusaba, T. Yagi, M. Kikuchi, and Y. Syono, J. Phys. Chem. Solids **47**, 675 (1986).
[24] Z. Mursic, T. Vogt, H. Boysen, and F. Frey, J. Appl. Crystallogr. **25**, 519 (1992).
[25] M. Marqués, M. Flórez, J. M. Recio, L. Gerward, and J. S. Olsen, Phys. Rev. B **74**, 014104 (2006).
[26] M. B. Smirnov, A. P. Mirgorodsky, V. Yu. Kazimirov, and R. Guinebretiere, Phys. Rev. B **78**, 094109 (2008).
[27] I. Farnan, E. Balan, C. J. Pickard, and F. Mauri, Am. Mineral. **88**, 1663 (2003).
[28] J.-P. Crocombette and D. Ghaleb, J. Nucl. Mater. **257**, 282 (1998).
[29] A. Korkin, H. Kamisaka, K. Yamashita, A. Safonov, and A. Bagatur'yants, Appl. Phys. Lett. **88**, 181913 (2006).
[30] S. Ono, Y. Tange, I. Katayama, and T. Kikegawa, Am. Mineral. **89**, 185 (2004).
[31] H. Özkan and J. C. Jamieson, Phys. Chem. Miner. **2**, 215 (1978).
[32] R. M. Hazen and L. W. Finger, Am. Mineral. **64**, 196 (1979).
[33] G.-M. Rignanese, F. Detraux, X. Gonze, and A. Pasquarello, Phys. Rev. B **64**, 134301 (2001).
[34] M. Zhang, L. A. Boatner, E. K. H. Salje, R. C. Ewing, P. Daniel, W. J. Weber, Y. Zhang, and I. Farnan, Phys. Rev. B **77**, 144110 (2008).
[35] R. M. Badger, J. Chem. Phys. **2**, 128 (1934).
[36] S. J. Duclos, A. Jayaraman, G. P. Espinosa, A. S. Cooper, and R. G. Maines, Sr., J. Phys. Chem. Solids **50**, 769 (1989).
[37] A. Jayaraman, G. A. Kourouklis, G. P. Espinosa, A. S. Cooper, and L. G. Van Uitert, J. Phys. Chem. Solids **48**, 755 (1987).
[38] Y. W. Long, L. X. Yang, Y. Yu, F. Y. Li, Y. X. Lu, R. C. Yu, Y. L. Liu, and C. Q. Jin, J. Appl. Phys. **103**, 093542 (2008).
[39] M. B. Smirnov and A. P. Mirgorodsky, in *Vibrations of Oxide Lattices*, edited by A. N. Lazarev (Nauka, Leningrad, 1980), p. 100.
[40] D. A. Kleinman and W. G. Spitzer, Phys. Rev. **125**, 16 (1962).
[41] C. Pecharromán, M. Ocaña, P. Tartaj, and C. J. Serna, Mater. Res. Bull. **29**, 417 (1994).
[42] F. Gervais, B. Piriou, and F. Cabannes, J. Phys. Chem. Solids **34**, 1785 (1973).